IEEE Access
Multidisciplinary | Rapid Review | Open Access Journal

Received 11 June 2024, accepted 8 July 2024, date of publication 11 July 2024, date of current version 22 July 2024.

Digital Object Identifier 10.1109/ACCESS.2024.3426941

RESEARCH ARTICLE

Adaptive Laplacian Continuous Mixed-Norm Control Approach for Dynamic Performance Improvement of Wind Energy Systems

AYEDH H. ALQAHTANI[1], (Senior Member, IEEE), HANY M. HASANIEN[2,3], (Senior Member, IEEE), MOHAMMED ALHARBI[4], SUN CHUANYU[5], (Member, IEEE), AND S. M. MUYEEN[6], (Fellow, IEEE)

[1]Department of Electrical Engineering, College of Technological Studies, The Public Authority for Applied Education and Training, Safat 23167, Kuwait
[2]Electrical Power and Machines Department, Faculty of Engineering, Ain Shams University, Cairo 11517, Egypt
[3]Faculty of Engineering and Technology, Future University in Egypt, Cairo 11835, Egypt
[4]Department of Electrical Engineering, College of Engineering, King Saud University, Riyadh 11421, Saudi Arabia
[5]School of Electrical Engineering and Automation, Harbin Institute of Technology, Harbin 150006, China
[6]Department of Electrical Engineering, Qatar University, Doha, Qatar

Corresponding author: Hany M. Hasanien (hanyhasanien@ieee.org)

This work was supported by King Saud University, Riyadh, Saudi Arabia, through the Researchers Supporting Project under Grant RSP2024R467.

ABSTRACT This paper introduces an adaptive filtering algorithm based on the Laplacian continuous mixed-norm (LCMN) as a control methodology to improve both transient and dynamic wind energy systems (WESs) performances. The foundation of this wind system is a variable-speed wind turbine that powers a permanent magnet synchronous generator. The proposed LCMN algorithm automatically updates all interface circuits' proportional-integral (PI) controllers gains. It has several advantages compared with other algorithms such as higher algorithm stability, lower fluctuations and steady-state errors. The efficacy of the LCMN-based PI control approach is validated by a fair comparison with other control methods such as the least mean square, robust mixed norm and continuous mixed p-norm when the WES is subjected to severe symmetrical and various unbalanced conditions. Furthermore, the applicability of the suggested technique is examined in typical operational circumstances utilizing actual wind speed measurements obtained from Hokkaido Island. The results indicate preferable performance of dynamic analyses even though the wind speed profile is intermittent.. The dynamic responses exhibit an actuating error of less than 2% across numerous profiles. Therefore, the LCMN-based PI control methodology is considered as an effective solution for online adjustment of controller gains in the course of system nonlinearities and uncertainties. A key advantage of this method is its independence from constructing system transfer functions and the avoidance of optimization methods. This can save substantial time and effort typically required for optimization processes.

INDEX TERMS Adaptive control, power system dynamics, renewable energy, wind energy systems.

I. INTRODUCTION

It is rigidly established that the global average temperature is on a steady rise increasing by 1.5°C due to emissions of greenhouse gases. This upward trend in temperature or

The associate editor coordinating the review of this manuscript and approving it for publication was R. K. Saket.

climate change triggers various environmental concerns [1]. Therefore, net-zero emissions or decarbonization poses a significant challenge for nations around the globe. The shift to renewable energy systems is crucial for meeting this goal. However, this transition is met with numerous hurdles including unadaptable regulatory and administrative processes for renewable energy projects, grid infrastructure that is not yet prepared and several technical difficulties. It is documented that wind energy ranks as the second most prominent source of renewable energy following hydro energy. In 2022, wind energy saw an addition of 78 GW in new capacity bringing the total global capacity to 906 GW by an annual growth of 9% [2]. To satisfy energy transition targets, wind energy shall be put on track and contribute to 20% of the world's electricity by 2030 with expectations set for it to account for one-third of global electricity by 2050 [2]. However, various technical challenges may arise due to escalating penetration of wind energy into power grids [3], [4], [5], [6]. A major concern is the impact on power system stability and reliability during severe disturbances in the wind energy system [3]. To address this, utilities have implemented grid codes requiring wind energy systems to connect to the power system and provide support during grid faults. Therefore, wind energy systems should satisfy the low voltage ride through (LVRT) capability requirements and support the grid under such conditions [7], [8]. To accomplish these objectives, advanced control strategies must be deployed to manage the interface circuits of wind energy systems thereby improving their transient and dynamic responses. These strategies are essential for mitigating the effects of wind energy uncertainty and nonlinearity caused by the intermittent nature of wind speed.

At the present time, fixed-speed wind generators are becoming less dominant in industrial applications [9], [10]. Generally, the trend in wind turbine development and deployment clearly favors variable-speed generators for their technological and operational benefits. They possess advanced control strategies, lower mechanical stress on their shafts, reduced power fluctuations and higher efficiency [11], [12], [13], [14]. The market features a variety of these generators including doubly-fed induction generators [7], [15], [16], permanent magnet synchronous generators (PMSGs) [17], [18], [19] and switched reluctance generators [20], [21], [22], [23] among others. Notably, PMSGs are commonly used as direct drive wind generators in various wind farms for several reasons: 1) they have larger diameters more magnetic poles and wider air gaps; 2) they operate at lower rotational speeds; and 3) they do not require a gearbox to connect the wind turbine with the generator which leads to lower costs and mechanical losses. This study focuses on a PMSG that is connected into the power grid via a grid side inverter (GSI), a DC-link capacitor and a generator side converter (GSC).

In a broad sense, the cascaded or vector control method is implemented to control both the GSC and GSI. In these negative feedback control systems, the traditional proportional plus integral (PI) controller is utilized knowing for their broad stability range. However, the PI controller suffers from the nonlinear nature of the system and is highly sensitive to changes in parameters values. Moreover, it is significantly challenging to obtain transfer functions of WESs due to the system's nonlinearity and the intermittent nature of wind speed. Therefore, various studies have been conducted to optimally design PI controllers of interface circuits for such systems. In [24], genetic algorithms were employed to fully devise PI controllers to enhance the performance of WESs. The Taguchi method has been used analytically for controller design in [25] and several metaheuristic optimization algorithms have been adopted to minimize the integral square error objective function to yield the optimal design of the controllers for LVRT capability and dynamic responses including improved grey wolf [8], salp swarm optimizer [26], transient search algorithm [27] among others [28], [29], [30], [31], [32]. Despite the fundamental achievements of these metaheuristic algorithms in getting the optimal gains of the controllers, they encounter issues such as complicated mathematical operations, prolonged processing times and powerful memory requirements. In addition, to boost WESs' LVRT, discharge resistance with rotor storage has been implemented in [33]. Techniques such as dumping resistance, superconducting magnetic energy storage (SMES) and supercapacitors have been explored in [34] for LVRT improvements. SMES combined with unified power flow controllers is utilized for power smoothing and LVRT enhancement [16]. In [35], the partial feedback linearization method has been adopted to further enhance LVRT. However, many PI controller designs rely on trial and error, a process that is both intricate and time-consuming. Moreover, fuzzy logic controllers (FLCs) are extensively used to control converter circuits improving LVRT and dynamic performance of WESs [36], [37], [38], [39] though reliant on the designer's experience in selecting fuzzy sets and memberships. Artificial Neural Network (ANN) controllers are also used to stabilize the output power of wind farms and enhance LVRT capabilities [40], [41] requiring extensive training and testing periods. Sliding mode control has been implemented to mitigate wind power fluctuations [42]. In addition, several adaptive control schemes are used for converter regulation to improve LVRT and overall WESs performance, such as affine projection [43], least mean square (LMS) exponential root [12], adaptive Bayesian [3] and hybrid adaptation algorithms [44]. These techniques focus on updating controllers in real-time to achieve optimal performance thereby potentially saving extensive time and effort when optimization is not required.

This paper proposes a cutting-edge application of an adaptive filtering algorithm called Laplace continuous mixed norm (LCMN) to update the controller gains for the interface circuits of WESs. The primary goal is to improve the LVRT capability and the dynamic response of WESs. To ensure realistic dynamic analyses, wind speed data from Hokkaido Island were incorporated. The setup involves PMSG driven by a wind turbine tied to the power grid via a GSC, DC-link

capacitor and a GSI. A cascaded or vector control scheme is employed to control both converters incorporating an LCMN-based PI control method. The GSC focuses on maximizing power output and managing reactive power whereas the GSI's role is to regulate voltage at the point of common coupling (PCC), maintain DC-link voltage stability and control inverter currents. The proposed adaptive LCMN filtering algorithm stands out by offering enhanced stability, reduced fluctuations and minimized steady-state errors over other algorithms. It operates primarily on the error signal, input vector and utilizes the Laplacian exponential function. The validity of the suggested methodology has been proved through its performance under both symmetrical and asymmetrical fault conditions serving as network disturbances. Validation of the WES's dynamic response is further supported by actual wind speed data. The LCMN approach shows distinct advantages over other adaptive algorithms, including LMS, robust mixed norm (RMN) and continuous mixed p-norm (CMPN) with comprehensive results analyzed through PSCAD software. Consequently, the adaptive LCMN-PI control scheme significantly improves the transient and dynamic responses of WESs.

The structure of the paper is as follows: Section II introduces the modeling of variable-speed wind turbines. Section III explains the modeling of WES's. Section IV demonstrates the interface circuits and their control schemes. Section V introduces the proposed LCMN adaptive filtering algorithm. Section VI investigates the detailed results and discussion. The conclusion and recommendations for further research are provided in Section VII.

II. MODELING OF WIND TURBINES

The wind power driven by a wind turbine (P_M) is mathematically formulated by the following expression [37]:

$$P_M = 0.5\rho\pi r^2 V_w^3 C_P(\lambda, \beta) \tag{1}$$

where ρ stands for air density, r represents blade length (radius of turbine swept area), V_w^3 is the cubic wind speed, C_P refers to rotor efficiency or power coefficient and is a function of blade angle β *and* tip speed ratio λ The following equations are used to formulate C_P:

$$\lambda = \frac{\omega_r r}{V_W} \tag{2}$$

$$L_i = \frac{1}{\frac{1}{(\lambda+0.02\beta)} - \frac{0.03}{(\beta^3+1)}} \tag{3}$$

$$C_P(\lambda, \beta) = 0.73\left\{\frac{151}{L_i} - 0.58\beta - 0.002\beta^{2.14} - 13.2\right\} e^{\frac{-18.4}{L_i}} \tag{4}$$

where ω_r stands for shaft angular velocity.

Generally, the most widely utilized wind generators are thought to be variable-speed models due to their advanced control strategies, lower mechanical stress on turbines shafts, lower power fluctuations and higher efficiency. These variable-speed turbines are capable of harnessing maximum power across a broad range of wind speeds. To achieve this, Maximum Power Point Tracking (MPPT) techniques are employed enabling the capture of peak power in any wind condition within the operational range from cut-in to rated wind speeds. Fig. 1 illustrates the critical curves of the wind turbine indicating the locus of maximum power captured from the wind turbine. Given the complexities involved in measuring wind speed directly, the maximum power output is determined as follows [45]:

$$P_{max} = 0.5\rho\pi r^2 \left(\frac{\omega_r r}{\lambda_{opt}}\right)^3 C_{p-opt} \tag{5}$$

where C_{p-opt} stands for an optimal value of C_P and λ_{opt} represents an optimal value of λ. P_{max} serves as the reference power for controlling the GSC. When the rotor speed exceeds this threshold, the blade pitch angle control scheme kicks in to keep it at its rated value. There is no need to use a gearbox to couple the wind turbine with the PMSG as the generator is capable of running at lower speeds.

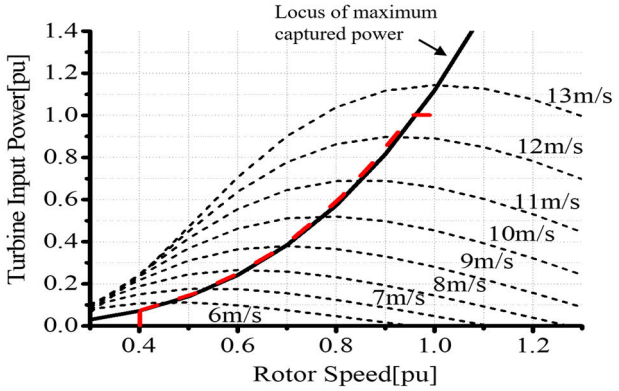

FIGURE 1. Wind turbine curves [43].

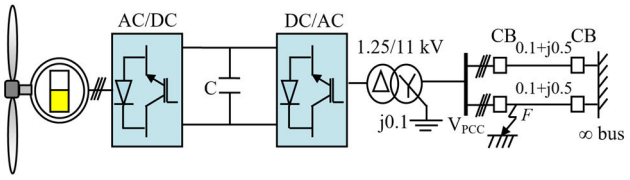

FIGURE 2. System model [43].

TABLE 1. PMSG specifications.

Rated power	5 MW	Stator resistance	0.01 p.u
Rated voltage	1.0 kV	d-axis reactance	1.0 p.u
Frequency	20 Hz	q-axis reactance	0.7 p.u
Poles	150	Magnetic flux	1.4 p.u
H	3 s		

III. SYSTEM UNDER STUDY AND PMSG DATA

Fig. 2 indicates the connection between the wind energy system and the power grid. The wind generation system consists of a PMSG driven by a variable-speed wind turbine. The wind generator can be tied to the grid through the transmission lines, a step-up transformer, GSI, DC-link capacitor and GSC. Both converters (GSC and GSI) are fully controlled through

the proposed LCMN-based PI control method. The wind generator specifications are listed in detail in Table 1. The base apparent power and system frequency are considered 5 MVA and 50 Hz respectively.

IV. INTERFACE CIRCUITS AND CONTROL

A. GENERATOR SIDE CONVERTER

The GSC functions as a three-phase controlled rectifier with six electronic switches, aimed at achieving MPPT for the WES across varying wind speeds. Utilizing a cascaded or vector control approach, as illustrated in Fig. 3, it meets its control objectives. There are two outer negative feedback control loops for regulating the reactive and active power of the wind generator. The first loop can effectively control the generator's active power to align with the MPPT condition, where P_{opt} and P_g represent the maximum and actual generator active power respectively. The second loop adjusts the generator's reactive power to ensure operation at a unity power factor with Q_{ref-g} and Q_g denoting the reference and actual generator reactive power respectively. Moreover, there are two inner negative feedback control loops for controlling the wind generator currents in direct and quadrature axis frames (I_d and I_q). Four adaptive filtering LCMN-based PI controllers are utilized in the presented control strategy to yield the control objectives. Output reference voltage signals V_{dref} and V_{qref} are transformed from the dq0 to abc reference frame using the generator angular displacement θ_r. These signals are then compared against a triangular waveform to generate delay pulses for the insulated gate bipolar transistor (IGBT) switches with a triangular carrier frequency set at 1kHz for simulation purposes.

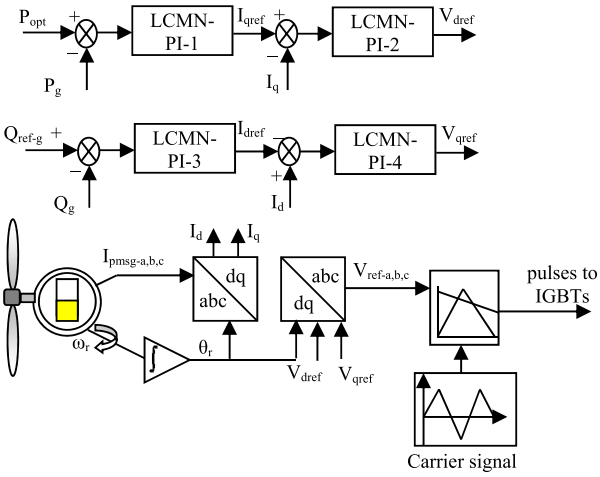

FIGURE 3. Detailed control of GSC.

B. GRID SIDE INVERTER

The GSI is designed as a three-phase, two-level inverter circuit featuring six electronic switches with its control objectives achieved through a cascaded or vector control strategy, as shown in Fig. 4. It incorporates two outer negative feedback control loops for controlling the DC-link and PCC voltages (V_{DC} and V_{PCC}) respectively. In addition, two inner negative feedback control loops are dedicated for controlling the currents at the PCC in direct and quadrature axis frames (I_{dn} and I_{qn}). In the presented control strategy, four adaptive filtering LCMN-based PI controllers are employed to yield the control objectives. Output reference voltage signals V_{dnref} and V_{qnref} are transformed from the dq0 to abc reference frame using the transformation angle θ_t which can be extracted by following the voltage signals V_{PCC} to a phase-locked loop (PLL) circuit. These signals are then compared to a triangular waveform to produce delay pulses for the six IGBTs with a carrier frequency for the triangular waveform set at 1 kHz for simulation purposes. The proposed LCMN and other adaptive algorithms are described in the next section.

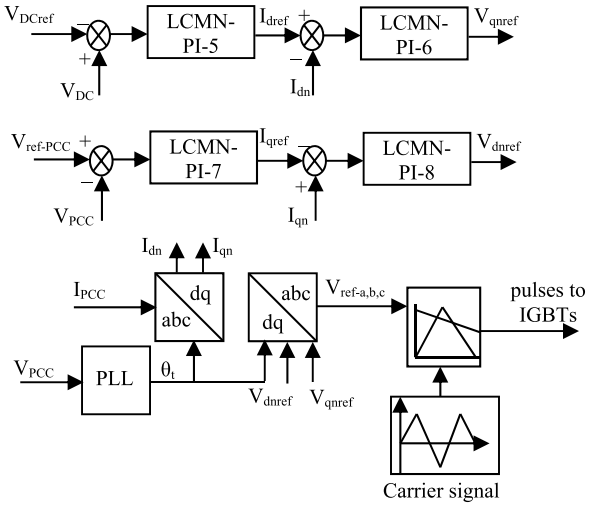

FIGURE 4. Detailed control of the GSI.

V. ADAPTIVE FILTERING ALGORITHMS

Adaptive filtering algorithms (AFAs) are dynamic algorithms designed to adjust variables in real-time to meet specific control objectives. These algorithms are widely applied to diverse industrial usages such as system identification, noise blocking, communication and electronics, and data-driven analysis [3]. The core function of these algorithms is to minimize the error between the reference and the actual signals by continous weight vector updates. AFAs come in various forms each distihuished by its algorithm methodology or computational procedure.

A. LEAST MEAN SQUARE

The least mean square (LMS) algorithm stands out as a mature type of AFAs renowned for its broad application spectrum. It is characterized by straightforward procedures and minimal memory requirements. These merits have an impact on the algorithm's accuracy and robustness. The weight vector of the LMS algorithm is defined as follows [3]:

$$w(i+1) = w(i) + \mu e(i)x(i) \tag{6}$$

where μ stands for a small value, $e(i)$ is the actuating error signal, i refers to the iteration index and $x(i)$ represents the

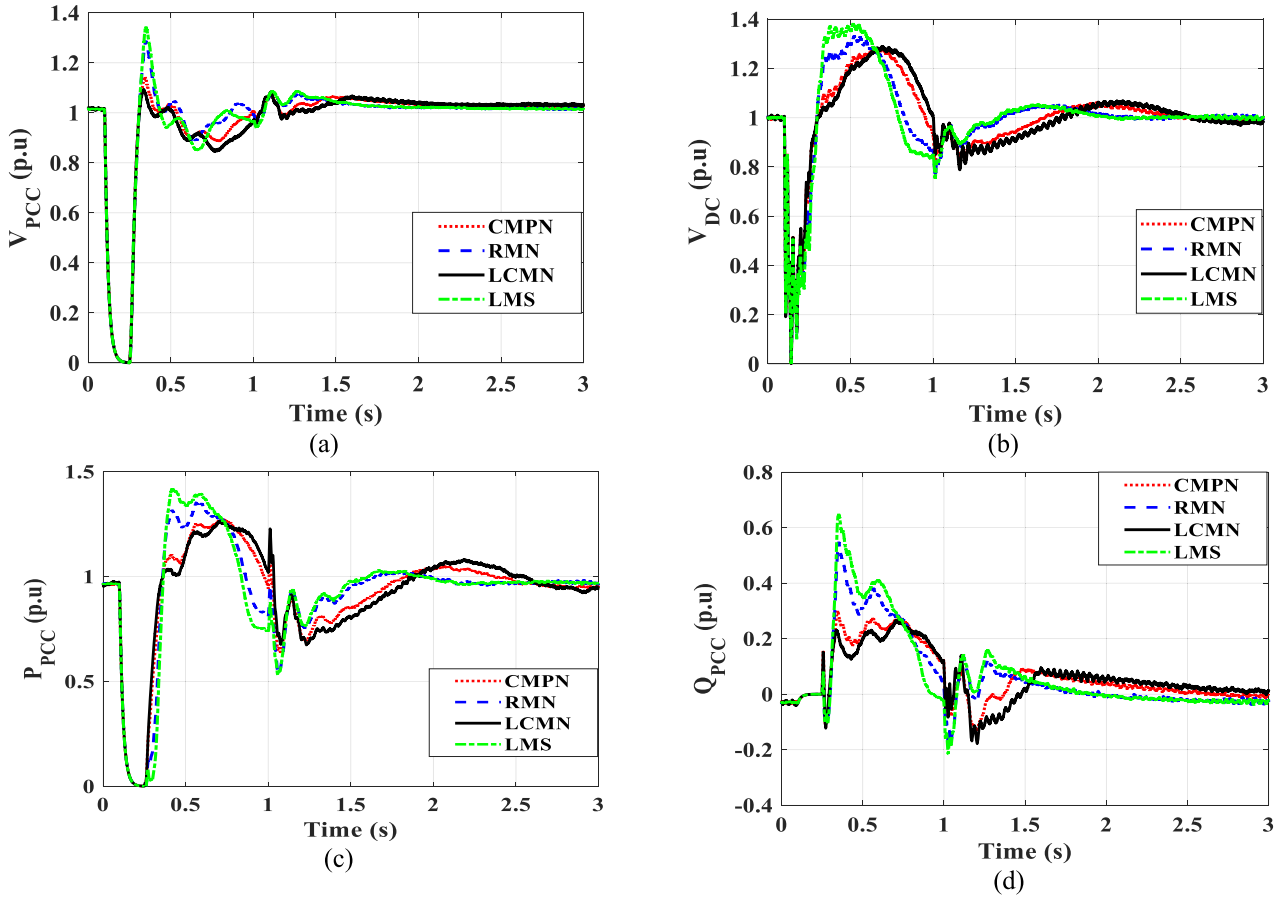

FIGURE 5. Transient responses due to 3LG fault conditions. (a) V_{PCC}. (b) V_{DC}. (c) P_{PCC}. (d) Q_{PCC}.

input vector. The gains of the PI controller are dynamically adjusted in real-time using the equation below:

$$\Delta k_p(i) = \Delta k_i(i) = \mu e(i) x(i) \tag{7}$$

B. ROBUST MIXED NORM

The robust mixed norm (RMN) methodology merges the merits of the LMS and the least absolute error deviation approaches. Its cost function can be described as follows:

$$C(i) = L(i) E\left\{e^2(i)\right\} + (1 - L(i)) E\{|e(i)|\} \tag{8}$$

where L regulates error norms in the range 0 and 1. The weight vector of the RMN algorithm is defined as follows:

$$w(i+1) = w(i) + \mu_1 e^2(i) .x(i) + \mu_2 |e(i)| .x(i) \tag{9}$$

where, μ_1 and μ_2 are small step sizes. The gains of the PI controller are modified in real-time through the following formula:

$$\Delta k_p(i) = \mu_1 e^2(i) .x(i) + \mu_2 \lfloor e(i) \rfloor .x(i) \tag{10}$$

$$\Delta k_i(i) = \mu_1 e^2(i) .x(i) + \mu_2 \lfloor e(i) \rfloor .x(i) \tag{11}$$

C. CONTINUOUS MIXED P-NORM

The continuous mixed p-norm (CMPN) approach is one of the powerful AFAs. Throughout the control process, the error norm is subject to change. The CMPN approach features a p-norm expressed as follows [44]:

$$J(i) = \int_1^2 \lambda_i(p) E\left\{|e(i)|^p\right\} dp \tag{12}$$

where λ_i refers to a probability density function constrained in the manner described as follows:

$$\int_1^2 \lambda_i(p) dp = 1 \tag{13}$$

The following equation can be used to update the CMPN algorithm's weight vector:

$$w(i+1) = w(i) + \mu \gamma_i sign(e(i)) x(i) \tag{14}$$

where γ_i stands for the step size and it is a function of $e(i)$. γ_i can be mathematically modeled as follows:

$$\gamma_i = \frac{(2|e(i)| - 1)\ln(|e(i)|) - |e(i)| + 1}{(\ln(e(i)))^2} \tag{15}$$

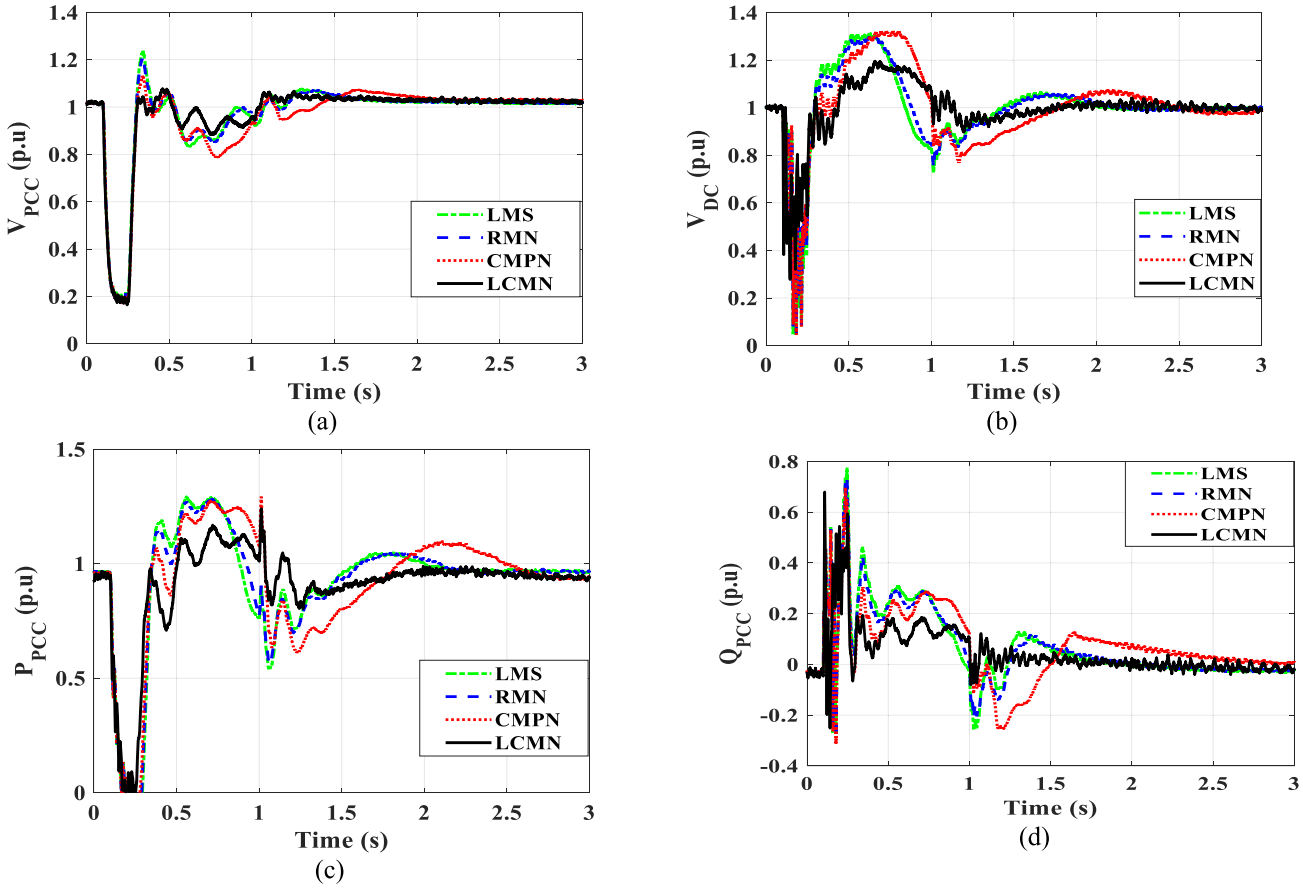

FIGURE 6. Transient responses due to 2LG fault conditions. (a) V_{PCC}. (b) V_{DC}. (c) P_{PCC}. (d) Q_{PCC}.

The gains of the PI controller are dynamically adjusted in real-time using the equation below:

$$\Delta k_p(i) = \Delta k_i(i) = \mu\gamma_i sign(e(i))\, x(i) \tag{16}$$

D. LAPLACIAN CONTINUOUS MIXED NORM

The Laplacian continuous mixed norm (LCMN) algorithm was introduced by Hadi Zayyani et al. in 2023 [46]. The term Laplacian is selected due to the similarity with the Laplace transform including algorithm derivation. The proposed LCMN relies mainly on the actuating error signal, input vector and the Laplacian exponential function. It offers multiple benefits over other algorithms, such as better algorithm stability, lower fluctuations and minimized steady-state errors [46].

The probability density function λ_i can be written as follows:

$$\lambda_i(p) = e^{-sp} \tag{17}$$

The LCMN approach applies a mixing-norm and its objective function is written as follows:

$$J(i) = \int_1^{\infty} e^{-sp} E\left\{|e(i)|^p\right\} dp \tag{18}$$

where s represents a decay factor of the density function. The p-norm can be extended from 1 to ∞. The following equation can update the weight vector of the LCMN algorithm:

$$w(i+1) = w(i) + \mu sign(e(i))\, f(e(i))x(i) \tag{19}$$

where the function $f(e(i))$ can be mathematically modeled as follows:

$$f(e(i)) = e^{-s}\frac{1 + s - \ln(|e(i)| + \epsilon)}{(s - \ln(|e(i)| + \epsilon))^2} \tag{20}$$

where s is a positive number chosen as 5 in the dynamic analysis to yield improved outcomes. ϵ represents a small positive value and equals 0.01. The following equations continuously adapt the PI controller gains:

$$k_p(i+1) = k_p(i) + \mu\, sign(e(i))\, f(e(i))x(i) \tag{21}$$

$$k_i(i+1) = k_i(i) + \mu\, sign(e(i))\, f(e(i))x(i) \tag{22}$$

In equations (21) and (22), $e(i)$ refers to the input signal of the PI controller, $x(i)$ stands for an actual signal that feeds the comparator and μ is 0.01. The initial values of these gains should be carefully selected to ensure the system's stability margin.

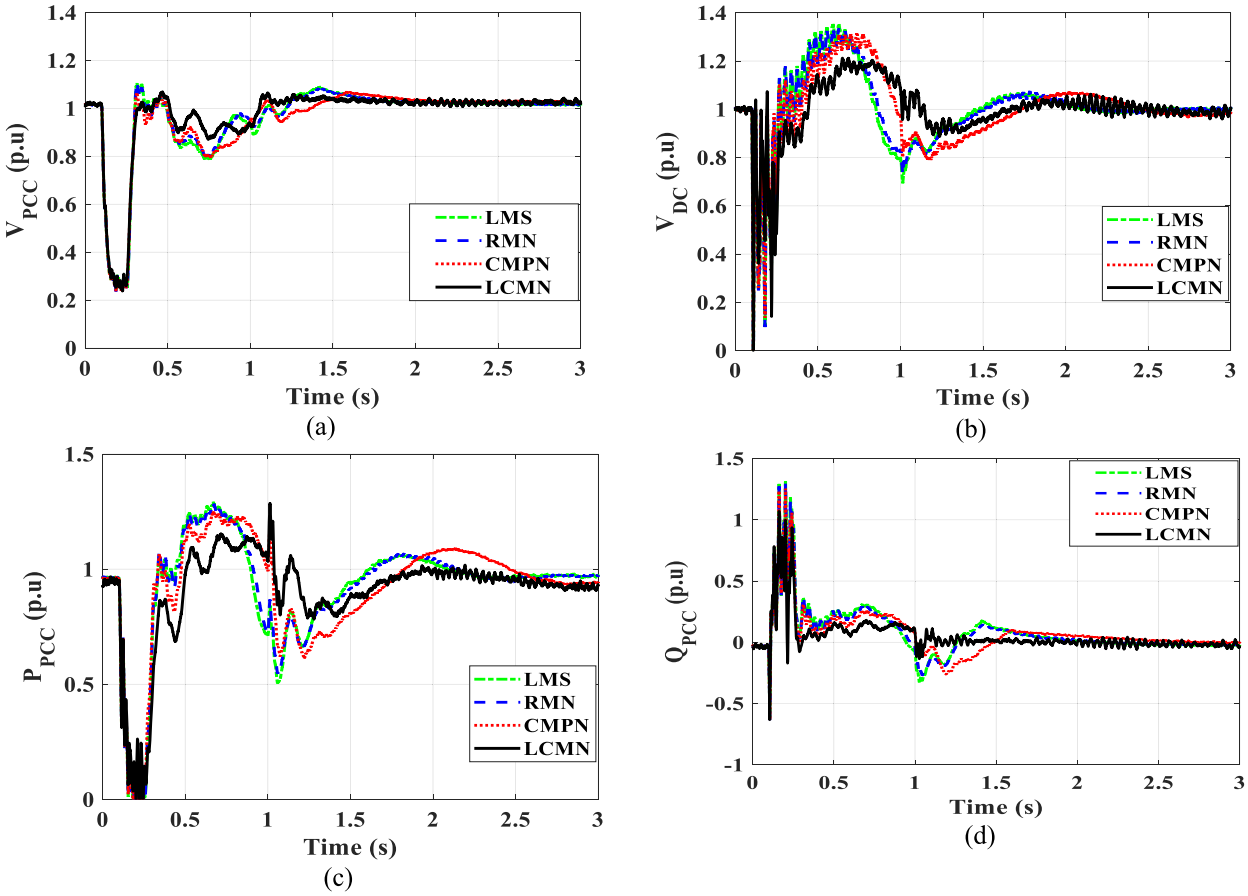

FIGURE 7. Transient responses due to LL fault conditions. (a) V_{PCC}. (b) V_{DC}. (c) P_{PCC}. (d) Q_{PCC}.

VI. SIMULATION RESULTS AND DISCUSSIONS

In this paper, a variable-speed wind turbine powers the PMSG directly and power converters (GSC and GSI) connect it to the grid. The whole system is mathematically modeled in detail incorporating all detailed electronic switches models. The system dynamics are carried out using PSCAD software [47]. The numerical analyses are performed using a PC of Intel Core Processor i7-9750H CPU @ 2.60GHz and its RAM is 32 GB. The transient and dynamic analyses of the system are performed under different conditions, as shown in the following subsections.

A. SCENARIO 1: TRANSIENT ANALYSES OF WIND ENERGY SYSTEMS

Scenario 1 details the transient analyses of the WES using the proposed control strategy. In this transient mode, wind speed is kept constant at its nominal value (12.4 m/s) showing no variation over a brief span of a few seconds. To investigate a realistic mode of operation, the time step of the simulation and channel plot time is selected to be 5 and 50 μs respectively. The WES is subjected to a symmetrical three-line to ground (3LG) fault condition at the instant t = 0.1 s on point F at the sending end of the transmission line, as depicted in Fig. 2 with the fault lasting for 0.1 s. The Circuit breakers (CBs) for the faulty line activate at t = 0.2 s to clear the fault and are reset to their normal state at t = 1 s. Fig. 5(a) demonstrates the V_{PCC} response dropping to zero due to the fault while the DC-link capacitor assists the grid with reactive power to improve the voltage profile. It should be noted that the voltage response using the LCMN-PI control scheme shows minimum fluctuations, lower overshoots and reduced steady state error when compared to other control techniques such as LMS, RMN, and CMPN-based PI controllers. The DC-link voltage profile is illustrated in Fig. 5(b) and exhibits a better-damped response using the LCMN-PI control scheme. Moreover, Fig. 5(c) and (d) show the transient responses of active and reactive power out of the PCC respectively. Notably, these profiles have lower undershoots, fewer overshoots, lower settling time and better transient specifications using the proposed adaptive methodology compared to other techniques. These overshoots or undershoots are reduced by more than 10% and 20% for the active and reactive power using the LCMN-PI control strategy compared with that obtained through the traditional LMS-based PI control method.

For obtaining further verification of the proposed methodology, the WES is subjected to various unsymmetrical fault conditions at the sending end of the transmission

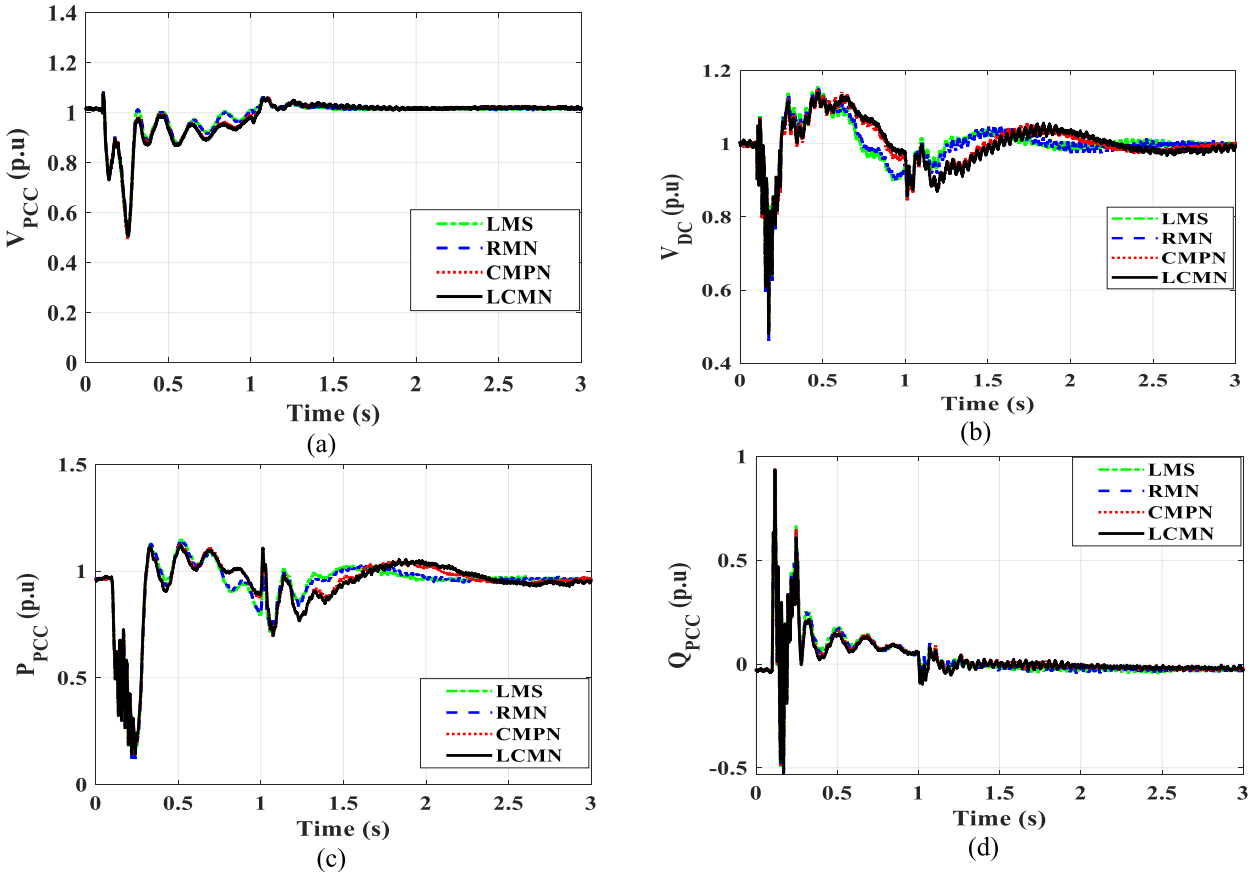

FIGURE 8. Transient responses due to 1LG fault conditions. (a) V_{PCC}. (b) V_{DC}. (c) P_{PCC}. (d) Q_{PCC}.

line, as demonstrated in Fig. 2. These faults are single-line-to-ground (1LG), line-line (LL) and double-line-to-ground (2LG). Figs. 6-8 illustrate the transient responses of PCC voltage, DC-link voltage and active and reactive powers under these unbalanced system conditions. In a similar manner, the transient profiles of all system responses using the LCMN-PI control strategy feature better damping and transient performances compared to other control methods. This can lead to outstanding transient performances attributable to the LCMN-PI control strategy.

B. SCENARIO 2: DYNAMIC ANALYSES OF WIND ENERGY SYSTEMS

Scenario 2 examines dynamic analyses of the WES at normal operating conditions using the proposed control strategy. For precise simulation outcomes, the time step of the simulation, simulation time, and channel plot time are selected to be 5 μs, 300 s and 50 μs, respectively. Moreover, measured wind speed profiles sourced from Hokkaido Island are incorporated into dynamic analyses providing a closer approximation to real-world conditions. Fig. 9(a) reveals the intermittent nature of the wind speed profile which ranges from 8.64 to 13.5 m/s indicating a wide range of speed variability. V_{PCC} and V_{DC} profiles are reported in Figs. 9(b) and (c). It is found that these responses are accurate and better damped with fluctuations less than 2% and 3% respectively lying in acceptable ranges of voltage dynamics using the proposed control method. Fig. 9(d) indicates the active power out of PCC during the normal operation of the WES. It can be noted that this active power does not reach 1 p.u at the PCC because of the power losses in interface components like GSC, GSI and the transformer. The role of the blade pitch angle controller is crucial in keeping the power within rated levels when wind speeds surpass nominal values with the blade angle adjustment ensuring operational requirements are met, as shown in Figure 9(e). Fig. 9(f) shows the dynamic performance of reactive power out of the PCC under normal operating conditions. It can be stated that the reactive power response satisfies a unity power factor operation despite the uncertainty and variability of wind speed based on the adaptive control method. It should be noted that dynamic profiles of all system responses employing the LCMN-PI control strategy guarantee better damping, lower ripples and minimum steady-state errors under normal operating conditions. This leads to enhanced performance in both transient and dynamic analysis under the LCMN-PI control framework.

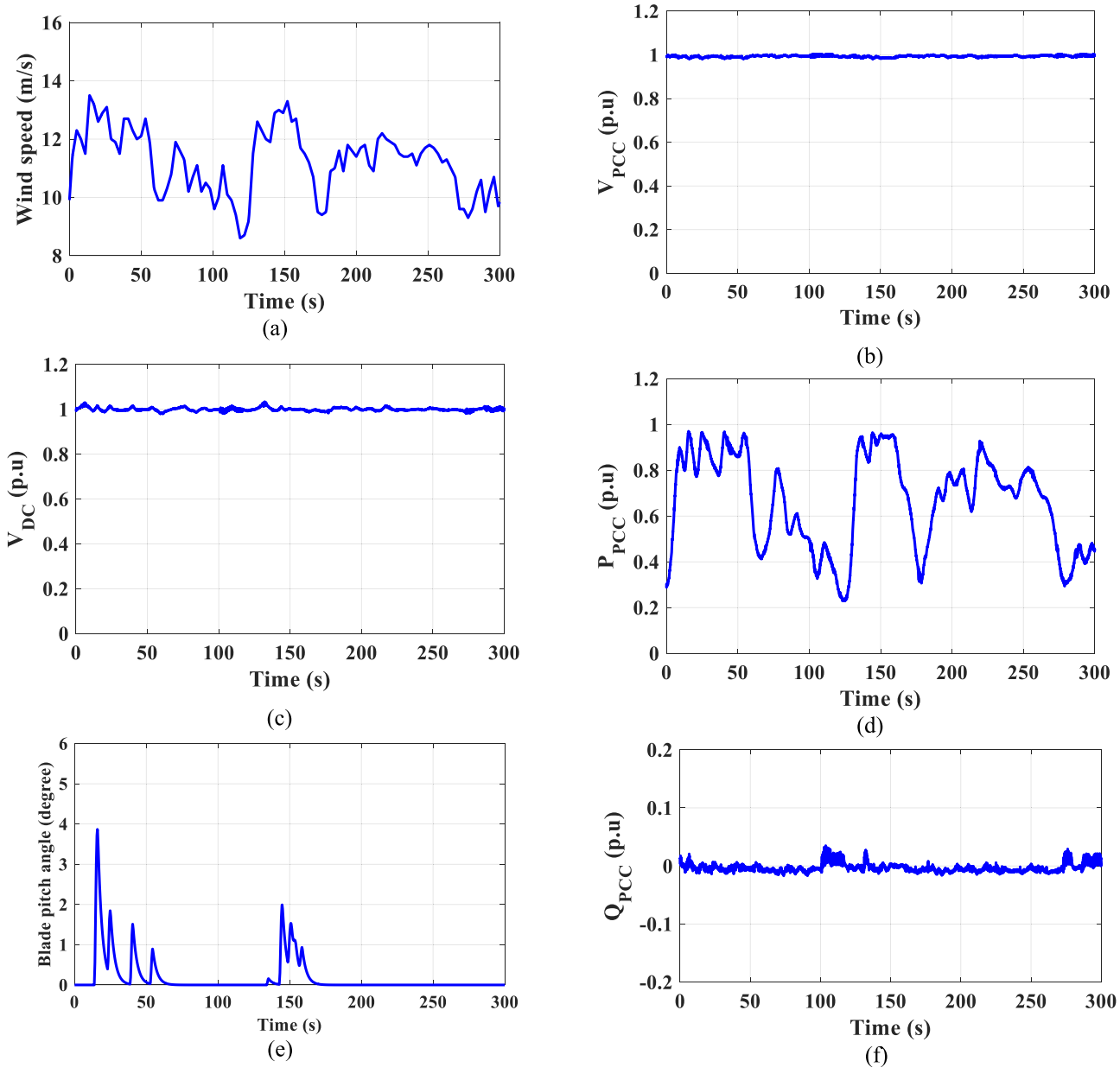

FIGURE 9. Dynamic responses under normal operating conditions and real wind speed data. (a) Wind speed. (b) V_{PCC}. (c) V_{DC}. (d) P_{PCC}. (e) Blade angle. (f) Q_{PCC}.

VII. CONCLUSION

This article has presented an adaptive LCMN-based PI control methodology enhancing both transient and dynamic grid-connected WESs analyses. The control method has been effectively integrated into the power converters within interface circuits. The effectiveness of the LCMN-based PI control methodology was validated by a fair comparison with other control methods like LMS, RMN and CMPN-based PI controllers when the WES is subjected to severe symmetrical and various unbalanced conditions. The numerical results revealed the high performance of the LCMN-based PI control methodology by achieving better transient response specifications showing more than 10% compared to the traditional LMS control method. Moreover, the validity of the proposed method was verified under normal operating conditions using measured real wind speed data displaying robust dynamic analyses despite the intermitted nature of the wind speed profile. The actuating error of these dynamic responses possesses less than 2% in many profiles. Therefore, the LCMN-based PI control methodology is considered an impressive approach for dynamically adjusting controller gains in the face of system uncertainties and nonlinearities. A key advantage of this approach is its independence from system transfer functions and optimization techniques. This, in fact, offers significant time and effort savings typically required by optimization processes. The proposed methodology presents a promising

option for wide range applications across different fields including other forms of renewable energy, microgrids, power system dynamics and smart grid technologies highlighting its potential for widespread impact.

ACKNOWLEDGMENT

This work was supported by the Researchers Supporting Project number (RSP2024R467), King Saud University, Riyadh, Saudi Arabia.

REFERENCES

[1] (2024). *COP28 UAE—United Nations Climate Change Conference*. Accessed: Mar. 09, 2024. [Online]. Available: https://www.cop28.com/en/

[2] (2023). *Global Wind Report 2023—Global Wind Energy Council*. Accessed: Mar. 09, 2024. [Online]. Available: https://gwec.net/globalwindreport2023/

[3] H. M. Hasanien, R. A. Turky, M. Tostado-Véliz, S. M. Muyeen, and F. Jurado, "Enhanced block-sparse adaptive Bayesian algorithm based control strategy of superconducting magnetic energy storage units for wind farms power ripple minimization," *J. Energy Storage*, vol. 50, Jun. 2022, Art. no. 104208, doi: 10.1016/j.est.2022.104208.

[4] P. T. H. Nguyen, S. Stüdli, J. H. Braslavsky, and R. H. Middleton, "Coordinated control for low voltage ride through in PMSG wind turbines," *IFAC-PapersOnLine*, vol. 51, no. 28, pp. 672–677, Jan. 2018, doi: 10.1016/j.ifacol.2018.11.782.

[5] J. Wei, C. Li, Q. Wu, B. Zhou, D. Xu, and S. Huang, "MPC-based DC-link voltage control for enhanced high-voltage ride-through of offshore DFIG wind turbine," *Int. J. Electr. Power Energy Syst.*, vol. 126, Mar. 2021, Art. no. 106591, doi: 10.1016/j.ijepes.2020.106591.

[6] D. Zholtayev, M. Rubagotti, and T. D. Do, "Adaptive super-twisting sliding mode control for maximum power point tracking of PMSG-based wind energy conversion systems," *Renew. Energy*, vol. 183, pp. 877–889, Jan. 2022, doi: 10.1016/j.renene.2021.11.055.

[7] A. Darvish Falehi and H. Torkaman, "Promoted supercapacitor control scheme based on robust fractional-order super-twisting sliding mode control for dynamic voltage restorer to enhance FRT and PQ capabilities of DFIG-based wind turbine," *J. Energy Storage*, vol. 42, Oct. 2021, Art. no. 102983, doi: 10.1016/j.est.2021.102983.

[8] M. H. Qais, H. M. Hasanien, and S. Alghuwainem, "Augmented grey wolf optimizer for grid-connected PMSG-based wind energy conversion systems," *Appl. Soft Comput.*, vol. 69, pp. 504–515, Aug. 2018, doi: 10.1016/j.asoc.2018.05.006.

[9] S. M. Muyeen, H. M. Hasanien, and A. Al-Durra, "Transient stability enhancement of wind farms connected to a multi-machine power system by using an adaptive ANN-controlled SMES," *Energy Convers. Manage.*, vol. 78, pp. 412–420, Feb. 2014, doi: 10.1016/j.enconman.2013.10.039.

[10] P. Sebastian and U. Nair, "Improved low voltage ride through capability of a fixed speed wind generator using dynamic voltage restorer," *Proc. Technol.*, vol. 25, pp. 767–774, Jan. 2016, doi: 10.1016/j.protcy.2016.08.171.

[11] A. Uehara, A. Pratap, T. Goya, T. Senjyu, A. Yona, N. Urasaki, and T. Funabashi, "A coordinated control method to smooth wind power fluctuations of a PMSG-based WECS," *IEEE Trans. Energy Convers.*, vol. 26, no. 2, pp. 550–558, Jun. 2011, doi: 10.1109/TEC.2011.2107912.

[12] M. H. Qais, H. M. Hasanien, and S. Alghuwainem, "A novel LMSRE-based adaptive PI control scheme for grid-integrated PMSG-based variable-speed wind turbine," *Int. J. Electr. Power Energy Syst.*, vol. 125, Feb. 2021, Art. no. 106505, doi: 10.1016/j.ijepes.2020.106505.

[13] N. Mughees, M. H. Jaffery, and M. Jawad, "A new predictive control strategy for improving operating performance of a permanent magnet synchronous generator-based wind energy and superconducting magnetic energy storage hybrid system integrated with grid," *J. Energy Storage*, vol. 55, Nov. 2022, Art. no. 105515, doi: 10.1016/j.est.2022.105515.

[14] H. Zhao, H. Zhou, W. Yao, Q. Zong, and J. Wen, "Multi-stage sequential network energy control for offshore AC asymmetric fault ride-through of MMC-HVDC system integrated offshore wind farms," *Int. J. Electr. Power Energy Syst.*, vol. 151, Sep. 2023, Art. no. 109180, doi: 10.1016/j.ijepes.2023.109180.

[15] C. R. Raghavendran, J. Preetha Roselyn, and D. Devaraj, "Development and performance analysis of intelligent fault ride through control scheme in the dynamic behaviour of grid connected DFIG based wind systems," *Energy Rep.*, vol. 6, pp. 2560–2576, Nov. 2020, doi: 10.1016/j.egyr.2020.07.015.

[16] J. X. Jin, R. H. Yang, R. T. Zhang, Y. J. Fan, Q. Xie, and X. Y. Chen, "Combined low voltage ride through and power smoothing control for DFIG/PMSG hybrid wind energy conversion system employing a SMES-based AC–DC unified power quality conditioner," *Int. J. Electr. Power Energy Syst.*, vol. 128, Jun. 2021, Art. no. 106733, doi: 10.1016/j.ijepes.2020.106733.

[17] H. The Nguyen, A. S. Al-Sumaiti, V.-P. Vu, A. Al-Durra, and T. D. Do, "Optimal power tracking of PMSG based wind energy conversion systems by constrained direct control with fast convergence rates," *Int. J. Electr. Power Energy Syst.*, vol. 118, Jun. 2020, Art. no. 105807, doi: 10.1016/j.ijepes.2019.105807.

[18] T. Yee Heng, T. Jian Ding, C. Choe Wei Chang, T. Jian Ping, H. Choon Yian, and M. Dahari, "Permanent magnet synchronous generator design optimization for wind energy conversion system: A review," *Energy Rep.*, vol. 8, pp. 277–282, Dec. 2022, doi: 10.1016/j.egyr.2022.10.239.

[19] D. E. Ghouraf, "An advanced control applied to PMSG wind energy conversion system implemented under graphical user interface," *Electr. Eng.*, vol. 105, no. 6, pp. 3841–3852, Dec. 2023.

[20] H. M. Hasanien and S. M. Muyeen, "Speed control of grid-connected switched reluctance generator driven by variable speed wind turbine using adaptive neural network controller," *Electric Power Syst. Res.*, vol. 84, no. 1, pp. 206–213, Mar. 2012, doi: 10.1016/j.epsr.2011.11.019.

[21] Z. Omaç and C. Cevahir, "Control of switched reluctance generator in wind power system application for variable speeds," *Ain Shams Eng. J.*, vol. 12, no. 3, pp. 2665–2672, Sep. 2021, doi: 10.1016/j.asej.2021.01.009.

[22] M. Makhad, K. Zazi, M. Zazi, and A. Loulijat, "Adaptive super-twisting terminal sliding mode control and LVRT capability for switched reluctance generator based wind energy conversion system," *Int. J. Electr. Power Energy Syst.*, vol. 141, Oct. 2022, Art. no. 108142, doi: 10.1016/j.ijepes.2022.108142.

[23] C. Liu, L. Wang, T. Zhang, X. Chen, and S. Ge, "Electromechanical dynamic analysis for powertrain of off-grid switched-reluctance wind turbine hydrogen production system," *Renew. Energy*, vol. 208, pp. 214–228, May 2023, doi: 10.1016/j.renene.2023.03.067.

[24] H. M. Hasanien and S. M. Muyeen, "Design optimization of controller parameters used in variable speed wind energy conversion system by genetic algorithms," *IEEE Trans. Sustain. Energy*, vol. 3, no. 2, pp. 200–208, Apr. 2012, doi: 10.1109/TSTE.2012.2182784.

[25] H. M. Hasanien and S. M. Muyeen, "A Taguchi approach for optimum design of proportional-integral controllers in cascaded control scheme," *IEEE Trans. Power Syst.*, vol. 28, no. 2, pp. 1636–1644, May 2013, doi: 10.1109/TPWRS.2012.2224385.

[26] M. H. Qais, H. M. Hasanien, and S. Alghuwainem, "Enhanced salp swarm algorithm: Application to variable speed wind generators," *Eng. Appl. Artif. Intell.*, vol. 80, pp. 82–96, Apr. 2019, doi: 10.1016/j.engappai.2019.01.011.

[27] M. H. Qais, H. M. Hasanien, and S. Alghuwainem, "Optimal transient search algorithm-based PI controllers for enhancing low voltage ride-through ability of grid-linked PMSG-based wind turbine," *Electronics*, vol. 9, no. 11, p. 1807, Oct. 2020, doi: 10.3390/electronics9111807.

[28] H. Kord, A.-A. Zamani, and S. M. Barakati, "Active hybrid energy storage management in a wind-dominated standalone system with robust fractional-order controller optimized by gases Brownian motion optimization algorithm," *J. Energy Storage*, vol. 66, Aug. 2023, Art. no. 107492, doi: 10.1016/j.est.2023.107492.

[29] H. Shukla and M. Raju, "Application of COOT algorithm optimized PID plus D2 controller for combined control of frequency and voltage considering renewable energy sources," *E-Prime-Adv. Electr. Eng., Electron. Energy*, vol. 6, Dec. 2023, Art. no. 100269, doi: 10.1016/j.prime.2023.100269.

[30] L. Yin and W. Ding, "Multi-objective high-dimensional multi-fractional-order optimization algorithm for multi-objective high-dimensional multi-fractional-order optimization controller parameters of doubly-fed induction generator-based wind turbines," *Eng. Appl. Artif. Intell.*, vol. 126, Nov. 2023, Art. no. 106929, doi: 10.1016/j.engappai.2023.106929.

[31] A. Daraz, "Optimized cascaded controller for frequency stabilization of marine microgrid system," *Appl. Energy*, vol. 350, Nov. 2023, Art. no. 121774, doi: 10.1016/j.apenergy.2023.121774.

[32] A. Saha, P. Dash, M. S. Bhaskar, D. Almakhles, and M. F. Elmorshedy, "Evaluation of renewable and energy storage system-based interlinked power system with artificial rabbit optimized PI(FOPD) cascaded controller," *Ain Shams Eng. J.*, vol. 15, no. 2, Feb. 2024, Art. no. 102389, doi: 10.1016/j.asej.2023.102389.

[33] J. Wang, Y. Ben, J. Zhang, and H. Feng, "Low voltage ride-through control strategy for a wind turbine with permanent magnet synchronous generator based on operating simultaneously of rotor energy storage and a discharging resistance," *Energy Rep.*, vol. 8, pp. 5861–5870, Nov. 2022, doi: 10.1016/j.egyr.2022.04.032.

[34] J. Tait, S. Wang, K. Ahmed, and G. P. Adam, "Comparative assessment of four low voltage fault ride through techniques (LVFRT) for wind energy conversion systems (WECSs)," *Alexandria Eng. J.*, vol. 61, no. 12, pp. 10463–10476, Dec. 2022, doi: 10.1016/j.aej.2022.04.003.

[35] M. A. Chowdhury, G. M. Shafiullah, and S. M. Ferdous, "Low voltage ride-through augmentation of DFIG wind turbines by simultaneous control of back-to-back converter using partial feedback linearization technique," *Int. J. Electr. Power Energy Syst.*, vol. 153, Nov. 2023, Art. no. 109394, doi: 10.1016/j.ijepes.2023.109394.

[36] K. A. Naik, C. P. Gupta, and E. Fernandez, "Design and implementation of interval type-2 fuzzy logic-PI based adaptive controller for DFIG based wind energy system," *Int. J. Electr. Power Energy Syst.*, vol. 115, Feb. 2020, Art. no. 105468, doi: 10.1016/j.ijepes.2019.105468.

[37] M. H. Qais, H. M. Hasanien, and S. Alghuwainem, "Whale optimization algorithm-based sugeno fuzzy logic controller for fault ride-through improvement of grid-connected variable speed wind generators," *Eng. Appl. Artif. Intell.*, vol. 87, Jan. 2020, Art. no. 103328, doi: 10.1016/j.engappai.2019.103328.

[38] A. Chakraborty and T. Maity, "An adaptive fuzzy logic control technique for LVRT enhancement of a grid-integrated DFIG-based wind energy conversion system," *ISA Trans.*, vol. 138, pp. 720–734, Jul. 2023, doi: 10.1016/j.isatra.2023.02.013.

[39] Y. Wang, Z. Wang, and H. Sheng, "Optimizing wind turbine integration in microgrids through enhanced multi-control of energy storage and micro-resources for enhanced stability," *J. Cleaner Prod.*, vol. 444, Mar. 2024, Art. no. 140965, doi: 10.1016/j.jclepro.2024.140965.

[40] F. Jamsheed and S. J. Iqbal, "An adaptive neural network-based controller to stabilize power oscillations in wind-integrated power systems," *IFAC-PapersOnLine*, vol. 55, no. 1, pp. 740–745, Jan. 2022, doi: 10.1016/j.ifacol.2022.04.121.

[41] M. Ding, Z. Tao, B. Hu, M. Ye, Y. Ou, and R. Yokoyama, "A fuzzy control and neural network based rotor speed controller for maximum power point tracking in permanent magnet synchronous wind power generation system," *Global Energy Interconnection*, vol. 6, no. 5, pp. 554–566, Oct. 2023, doi: 10.1016/j.gloei.2023.10.004.

[42] Y. Zhang, Y. Zhang, and T. Wu, "Integrated strategy for real-time wind power fluctuation mitigation and energy storage system control," *Global Energy Interconnection*, vol. 7, no. 1, pp. 71–81, Feb. 2024, doi: 10.1016/j.gloei.2024.01.007.

[43] H. M. Hasanien and S. M. Muyeen, "Affine projection algorithm based adaptive control scheme for operation of variable-speed wind generator," *IET Gener., Transmiss. Distribution*, vol. 9, no. 16, pp. 2611–2616, Dec. 2015, doi: 10.1049/iet-gtd.2014.1146.

[44] H. M. Hasanien, M. Tostado-Véliz, R. A. Turky, and F. Jurado, "Hybrid adaptive controlled flywheel energy storage units for transient stability improvement of wind farms," *J. Energy Storage*, vol. 54, Oct. 2022, Art. no. 105262, doi: 10.1016/j.est.2022.105262.

[45] S. M. Muyeen, R. Takahashi, T. Murata, and J. Tamura, "Control strategy for HVDC interconnected DC-based offshore wind farm," in *Proc. Int. Conf. Electr. Mach. Syst.*, Nov. 2009, pp. 1–6, doi: 10.1109/ICEMS.2009.5382777.

[46] H. Zayyani, M. Korki, and A. Taghavi, "A robust stable Laplace continuous mixed norm adaptive filter algorithm," *IEEE Sensors Lett.*, vol. 8, no. 3, pp. 1–4, Mar. 2024, doi: 10.1109/LSENS.2024.3370573.

[47] (2024). *V5 Features | PSCAD*. Accessed: Mar. 19, 2024. [Online]. Available: https://www.pscad.com/software/pscad/v5-features

AYEDH H. ALQAHTANI (Senior Member, IEEE) received the B.Sc. degree in electrical engineering from The University of North Carolina at Charlotte, Charlotte, NC, USA, in 2000, the M.Sc. degree from the University of Southern California, Los Angeles, CA, USA, in 2005, and the Ph.D. degree in electrical engineering from The Ohio State University, Columbus, OH, USA, in 2013. His current research interests include the integration of renewable energy into electric power systems, modeling and control of distributed energy generation, and the development of green energy systems. His contributions to the field are geared toward enhancing the sustainability and efficiency of energy systems.

HANY M. HASANIEN (Senior Member, IEEE) received the B.Sc., M.Sc., and Ph.D. degrees in electrical engineering from the Faculty of Engineering, Ain Shams University, Cairo, Egypt, in 1999, 2004, and 2007, respectively. From 2008 to 2011, he was a Joint Researcher with Kitami Institute of Technology, Kitami, Japan. From 2011 to 2015, he was an Associate Professor with the College of Engineering, King Saud University, Riyadh, Saudi Arabia. He is currently a Professor with the Electrical Power and Machines Department, Faculty of Engineering, Ain Shams University. He has authored, co-authored, and edited three books in the field of electric machines and renewable energy. He has published more than 300 papers in international journals and conferences. His research interests include modern control techniques, power systems dynamics and control, energy storage systems, renewable energy systems, and smart grids. He is an Editorial Board Member of *Electric Power Components and Systems*. His biography has been included in Marquis Who's Who in the World for its 28 edition, in 2011. He was awarded the Encouraging Egypt Award for Engineering Sciences, in 2012; the Institutions Egypt Award for Invention and Innovation of Renewable Energy Systems Development, in 2014; the Superiority Egypt Award for Engineering Sciences, in 2019; and the Ain Shams University Appreciation Award in Engineering Sciences, in 2022. He was the IEEE PES Egypt Chapter Chair (2020–2022). He is the Subject Editor of *IET Renewable Power Generation*, *Frontiers in Energy Research*, and *Electronics* (MDPI). He is also the Editor-in-Chief of *Ain Shams Engineering Journal* (Elsevier).

MOHAMMED ALHARBI received the B.S. degree in electrical engineering from King Saud University, Riyadh, Saudi Arabia, in 2010, the M.S. degree in electrical engineering from Missouri University of Science and Technology, Rolla, MO, USA, in 2014, and the Ph.D. degree in electrical engineering from North Carolina State University, Raleigh, NC, USA, in 2020. He was a Teaching Assistant with King Saud University, from September 2010 to May 2011. He was a Project Engineer with the FREEDM Systems Center, North Carolina State University, from January 2016 to December 2019, where he was involved in designing and constructing a modular multilevel converter for control validations. In August 2020, he joined the Department of Electrical Engineering, King Saud University, where he is currently an Assistant Professor. His research interests include medium voltage and high-power converters, modular multi-level converter (MMC) controls, multi-terminal HVdc systems, and grid integration of renewable energy systems.

SUN CHUANYU (Member, IEEE) received the bachelor's degree from Tianjin University, in 2012, the master's degree from Politecnico Di Milano, Italy, in 2014, and the Ph.D. degree from Università degli Studi di Padova, in 2019. Since October 2022, he has been an Associate Professor with the School of Electrical Engineering and Automation, Harbin Institute of Technology. His current research interests include fuel cells and redox flow batteries for large-scale energy storage applications, as well as their design, optimization, and modeling study.

S. M. MUYEEN (Fellow, IEEE) received the B.Sc. (Eng.) degree in electrical and electronic engineering from Rajshahi University of Engineering and Technology (RUET), Bangladesh, formerly known as Rajshahi Institute of Technology, in 2000, and the M.Eng. and Ph.D. degrees in electrical and electronic engineering from Kitami Institute of Technology, Japan, in 2005 and 2008, respectively. He is currently a Full Professor with the Electrical Engineering Department, Qatar University. His research interests include power system stability and control, electrical machines, FACTS, energy storage systems (ESS), renewable energy, and HVdc systems. He has been a keynote speaker and an invited speaker at many international conferences, workshops, and universities. He has published more than 350 articles in different journals and international conferences. He has published seven books as an author or an editor. He is serving as an Editor/Associate Editor for many prestigious journals from IEEE, IET, and other publishers, including IEEE TRANSACTIONS ON ENERGY CONVERSION, IEEE POWER ENGINEERING LETTERS, *IET Renewable Power Generation*, and *IET Generation, Transmission & Distribution*. He is also a Chartered Professional Engineer, Australia, and a fellow of Engineers Australia.